Int J Disaster Risk Sci (2021) 12:428–442
https://doi.org/10.1007/s13753-021-00349-3

www.ijdrs.com
www.springer.com/13753

ARTICLE

Mapping the Global-Scale Maize Drought Risk Under Climate Change Based on the GEPIC-Vulnerability-Risk Model

Yuanyuan Yin[1,2,3] · Yuan Gao[3] · Degen Lin[4] · Lei Wang[1,2,5] · Weidong Ma[6] · Jing'ai Wang[6,7]

Accepted: 13 April 2021 / Published online: 12 May 2021

Abstract Drought is projected to become more frequent and increasingly severe under climate change in many agriculturally important areas. However, few studies have assessed and mapped the future global crop drought risk—defined as the occurrence probability and likelihood of yield losses from drought—at high resolution. With support of the GEPIC-Vulnerability-Risk model, we propose an analytical framework to quantify and map the future global-scale maize drought risk at a 0.5° resolution. In this framework, the model can be calibrated and validated using datasets from in situ observations (for example, yield statistics, losses caused by drought) and the literature. Water stress and drought risk under climate change can then be simulated. To evaluate the applicability of the framework, a global-scale assessment of maize drought risk under 1.5 °C warming was conducted. At 1.5 °C warming, the maize drought risk is projected to be regionally variable (high in the midlatitudes and low in the tropics and subtropics), with only a minor negative (− 0.93%) impact on global maize yield. The results are consistent with previous studies of drought impacts on maize yield of major agricultural countries around the world. Therefore, the framework can act as a practical tool for global-scale, future-oriented crop drought risk assessment, and the results provide theoretical support for adaptive planning strategies for drought.

Keywords Climate change · Future-oriented risk assessment · GEPIC-Vulnerability-Risk model · Maize drought risk · Representative Concentration Pathway (RCP) scenarios

✉ Lei Wang
wanglei@itpcas.ac.cn

✉ Jing'ai Wang
jwang@bnu.edu.cn

[1] Key Laboratory of Tibetan Environment Changes and Land Surface Processes, Institute of Tibetan Plateau Research, Chinese Academy of Sciences (CAS), Beijing 100101, China

[2] CAS Center for Excellence in Tibetan Plateau Earth Sciences, Chinese Academy of Sciences (CAS), Beijing 100101, China

[3] School of Geography, Faculty of Geographical Science, Beijing Normal University, Beijing 100875, China

[4] College of Geography and Environmental Sciences, Zhejiang Normal University, Jinhua 321004, China

[5] University of Chinese Academy of Sciences, Beijing 100049, China

[6] School of Geographical Science, Qinghai Normal University, Xining 81008, China

[7] Faculty of Geographical Science, Beijing Normal University, Beijing 100875, China

1 Introduction

Frequent and severe droughts have affected nearly half of the world's countries, and are among the costliest natural hazards and disasters because of their destructive impact on crop growth and the agricultural economy (UNDP 2005; FAO 2015). As the climate warms, many agriculturally important areas of the world are likely to face increasingly frequent and serious droughts due to both reduced precipitation and increased evaporation (IPCC 2012, 2013; Dai 2013; Zeng et al. 2020). Drought-related losses to crop yield are projected to increase (Hoegh-Guldberg et al. 2018; Leng and Hall 2019). Drought risk assessment and mapping for future climate scenarios are therefore urgently needed so that effective adaptation and mitigation strategies can be implemented.

Over the past decades, future drought risk scenarios were only considered in 10% of drought risk assessments (Hagenlocher et al. 2019). Climate scenarios simulated by global climate models (GCMs) have been used to assess future agricultural drought risk at different spatial scales. Yue et al. (2018) assessed future wheat drought loss risk in China, and Webber et al. (2018) projected yield losses to maize and winter wheat attributable to drought stress in Europe. At the global scale, Leng and Hall (2019) developed a copula-based probabilistic model and investigated the risk of yield losses by the end of the twenty-first century for four major crops—wheat, maize, rice, and soybeans—due to drought in the 10 countries with greatest production. However, studies of global-scale, future-oriented agricultural drought risk assessment at the grid level are rare.

Risk assessments can be divided into three categories: qualitative, semi-quantitative, and quantitative (Shi 2012). Recently, there has been a shift from a qualitative or semi-quantitative approach to a quantitative approach (Schneiderbauer et al. 2017). However, few studies focus on the quantitative assessment of future-oriented agricultural drought risk because the data required for the risk assessment—hazard, exposure, vulnerability, and crop yield loss data—are difficult to obtain. Physically-based crop models, which integrate multiple processes and consider the impacts of both the environment and management practices (Thornley and Johnson 1990; Boote et al. 1996), have been employed to predict potential climate impacts on crops (Boote et al. 2013) and to identify the drivers of crop yield losses (Yu et al. 2018; Yue et al. 2018). Over the last several years, many global gridded crop models (GGCMs) (for example, GEPIC, pDSSAT, PEGASUS) have been developed to simulate crop yield and climate impacts at the global scale. The Global Gridded Crop Model Intercomparison (GGCMI), a project of the Agricultural Model Intercomparison and Improvement Project (AgMIP), used 12−15 models to simulate crop yield over the historical period from 1948 to 2012 under uniform changes in temperature and water levels (Elliott et al. 2015; Franke et al. 2020). The Inter-Sectoral Impact Model Inter-comparison Project (ISI-MIP) selected six GGCMs to quantitatively assess agricultural risks of climate change at different levels of global warming (Warszawski et al. 2014; Rosenzweig et al. 2017). Furthermore, using the GGCMs, the impacts of drought (water scarcity) on agricultural production were evaluated (Schewe et al. 2014; Wang et al. 2014), but not particularly from a risk assessment perspective.

Based on the GEPIC model (Liu 2009), we developed a large-scale crop drought risk assessment model—the GEPIC-Vulnerability-Risk (GEPIC-V-R) model (Yin et al. 2014)—and assessed the global-scale drought risk for maize (Yin et al. 2014; Guo et al. 2016), wheat, and rice (Wang et al. 2016), demonstrating that the model is a practical and valuable tool for assessing future agricultural drought risk. Maize (*Zea mays L.*) is the second most widely planted cereal in the world, exceeded only by wheat according to the Food and Agriculture Organization (FAO) 2017,[1] and can be grown under precipitation levels from 200 to 2,000 mm (Hartkamp et al. 2001; Ramirez-Cabral et al. 2017). Here, using the GEPIC-V-R model, an analytical framework to quantify and map future maize drought risk at a global scale was developed. The analytical framework was then applied and evaluated in a case study evaluating the global drought-driven risk of yield losses for maize in a world that is 1.5 °C warmer (UNFCCC 2015) than the pre-industrial period 1881−1910.

2 Analytical Framework

In this study, maize drought risk is defined as the occurrence probability of drought and the corresponding expectation or likelihood of yield losses attributable to drought. The risk is derived from three factors: hazard, exposure, and vulnerability (Cardona et al. 2012). We used the GEPIC-V-R model (Yin et al. 2014), which integrates ArcGIS with EPIC0509, to develop the assessment framework. The model runs on a grid with a spatial scale of 0.5° × 0.5°, and the drought exposure in each grid is set to unity. Drought risk (R) is the product of hazard (H) and vulnerability (V) (Eq. 1) (Yin et al. 2014):

$$R = f(H, V) = H\{\langle P, DHI\rangle\} \times V\{\langle L, DHI\rangle\} \quad (1)$$

where P denotes the probability of occurrence; DHI denotes the drought hazard index; L denotes the yield loss ratio; $H\{\langle P, DHI\rangle\}$ describes the relationship between P and DHI; and $V\{\langle L, DHI\rangle\}$ describes the relationship between L and DHI.

The analytical framework for maize drought risk assessment under a given climate change scenario comprises four steps (Fig. 1): (1) calibration and validation of the EPIC model; (2) establishment of the drought vulnerability curve; (3) evaluation of the GEPIC-V-R model; and (4) quantification of the maize drought risk under the given scenario. First, the most sensitive parameters—the lowest harvest index WSYF (water stress yield factor, the coefficient of maize yield sensitivity to water stress at the most critical stage of growth), the harvest index HI, and the energy conversion rate WA (the energy to biomass conversion factor)—are used to calibrate the regional crop

[1] http://www.fao.org/faostat/en/data.

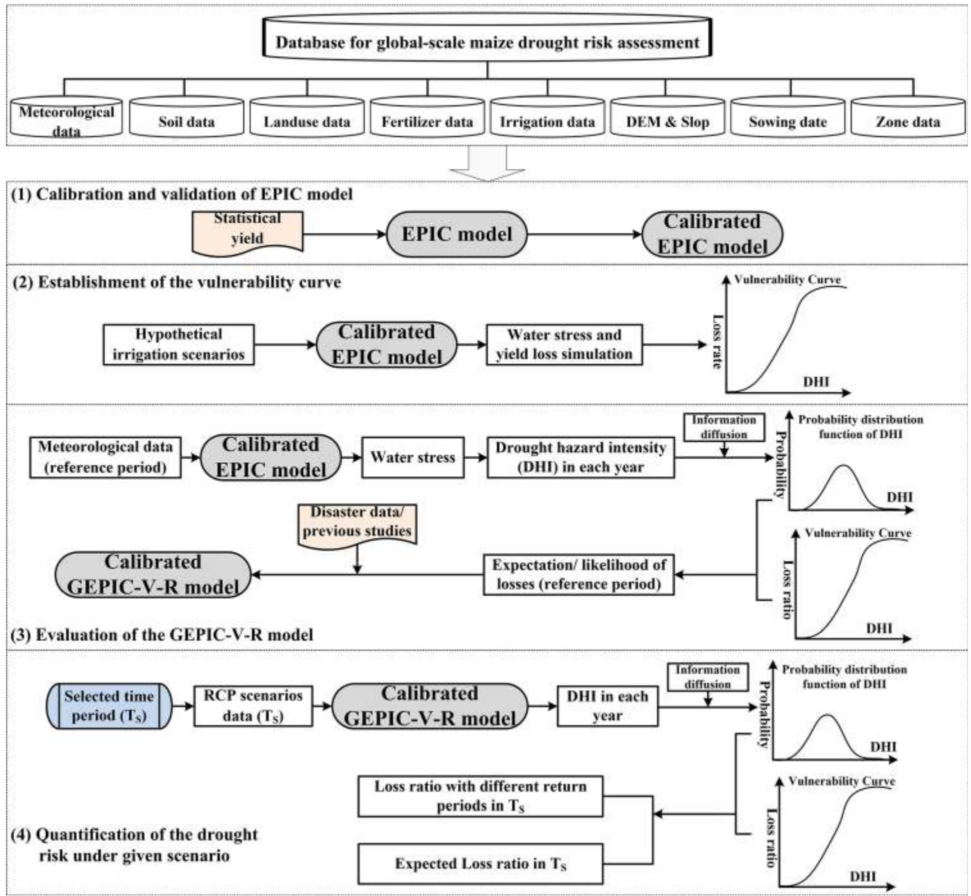

Fig. 1 Analytical framework for crop drought risk assessment under climate change based on the GEPIC-Vulnerability-Risk model

parameters by carefully comparing simulated yields with observed yields. Second, using the calibrated EPIC model, the drought stress and crop yield loss caused by water stress are calculated under a range of hypothetical irrigation scenarios, and drought vulnerability curves are fitted. Third, water stress during the maize growth period is simulated using the meteorological data to force the calibrated EPIC model for a reference period of 30 years. Then, the *DHI* and the maize yield loss ratio from drought in the reference period are calculated using the GEPIC-V-R model. Finally, the loss ratios simulated by the GEPIC-V-R model are compared to data from previously reported disasters as well as the literature, and the model skill is evaluated. Fourth, the *DHI* for a period in the future is simulated by forcing the GEPIC-V-R model with climate projections from GCMs, on the basis of Representative Concentration Pathway (RCP) scenarios to quantify the future maize drought risk over the selected period.

3 Data and Methods

According to the analytical framework, the soil, land use, DEM (digital elevation model), meteorological, agricultural, and loss data were required, and they are described in Sect. 3.1. Sections 3.2–3.5 detail the methods used in each step in the framework. In Sect. 3.6, the statistical analysis methods to investigate characteristics of the maize yield loss ratio from drought are presented.

3.1 Data

To simulate maize growth processes, the EPIC model inputs include soil, land use, DEM, meteorological, fertilizer, irrigation, and phenological data (Table 1). These data were mapped into a 0.5° grid using the methods detailed in Yin et al. (2014). Historical meteorological data, statistical maize yield data, data of losses caused by drought, and sown area data were used to calibrate and validate the EPIC model and to validate the GEPIC-V-R model. We determined the maize distribution by overlaying the layers of area of maize (Ramankutty et al. 2008) and the cropland. The cropland was extracted from the global land use and land cover data with ArcGIS.

Table 1 Data used in the analytical framework for crop drought risk assessment under climate change based on the GEPIC-Vulnerability-Risk model

Data	Content		Period, resolution/scale, and sources
Soil data	Soil type		2005, Food and Agriculture Organization (FAO)[2]
	Depth, percentage of sand, silt, and clay, soil bulk, PH, organic carbon content, calcium carbonate content		International Soil Reference and Information Centre—World Inventory of Soil Emission Potentials, 2000 (Batjes 2000)
Land-use data	Global land use		0.00833° × 0.00833°, United States Geological Survey (USGS)[3]
DEM data	Global DEM		0.0833° × 0.0833°, USGS[4]
Historical meteorological data	Daily mean temperature, minimum temperature, maximum temperature, solar radiation, precipitation, wind velocity, and relative humidity		1971–2004, 0.5° × 0.5°, Inter-Sectoral Impact Model Inter-comparison Project (ISI-MIP) (Warszawski et al. 2014)
Future meteorological data	Daily mean temperature, minimum temperature, maximum temperature, solar radiation, precipitation, wind velocity, and relative humidity		2005–2099, 0.5° × 0.5°, four RCP scenarios, ISI-MIP (Warszawski et al. 2014)
Agricultural data	Global fertilizer		1961–2002, country average, FAO[5]
	Global irrigation		2000, country average, Kassel University, Germany (Döll and Siebert 2002)
	Global maize sown date		World Agriculture Climate and Crops Climate (Cui 1994)
	Global statistical maize yield		1961–2010, country average, FAO[5]
	Sown area	Maize sown area	1978–2005, provincial, National Bureau of Statistics of China (NBSC)[6]
		Crop sown area	
Loss data	Covered areas, affected areas, and areas of total crop failure caused by drought in China		1978–2005, provincial, NBSC[6]

[2]http://www.fao.org/soils-portal/data-hub/soil-maps-and-databases/other-global-soil-maps-and-databases

[3]https://www.usgs.gov/centers/eros/science/usgs-eros-archive-land-cover-products-global-land-cover-characterization-glcc?qt-science_center_objects=0#qt-science_center_objects

[4]https://www.usgs.gov/centers/eros/science/usgs-eros-archive-digital-elevation-global-multi-resolution-terrain-elevation?qt-science_center_objects=0#qt-science_center_objects

[5]http://www.fao.org/faostat/en/#data/QC

[6]https://data.stats.gov.cn/english/easyquery.htm?cn=E0103

The bias-corrected and downscaled projection data for the period 2005–2099 for four RCP scenarios—RCP2.6, RCP4.5, RCP6.0, and RCP8.5 (van Vuuren et al. 2011)—were used to simulate the future *DHI* and assess the global drought risk of maize yield losses under climate change. The projected data were provided by ISI-MIP with a spatial resolution of 0.5° × 0.5° (Warszawski et al. 2014). Climate data from several Climate Model Inter-comparison Project Stage 5 (CMIP5) GCMs were provided by ISI-MIP. However, to reduce computational expense, we used only the HadGEM2-ES (Dike et al. 2015) simulations to demonstrate our framework for global assessment of drought risk to maize.

3.2 Calibration and Validation of the EPIC Model

Energy conversion rate (WA), harvest index (HI), and lowest harvest index (WSYF) were selected to calibrate the crop parameters for maize by carefully comparing the simulated yields with the observed yields. To improve the simulation accuracy at the global scale, the global maize-planting area was divided into 36 maize suitability zones (Yin et al. 2014). Because there were no maize-planting grids in the Oceania Tropical Irrigated Zone (Yin et al. 2014), the parameters for 35 maize suitability zones were calibrated. National maize yield statistics (2001–2003) from maize-planting countries around the world were used to validate the EPIC model. Figure 2 shows that there is a good linear relationship between the statistical and simulated yields. Four statistic indices were used to evaluate the statistical yields and the simulated yields—the Pearson correlation coefficient (R-square), root-mean-square error (RMSE), percent bias (PBIAS), and the Nash-Sutcliffe efficiency coefficient (NSE) (Fig. 2). The values of R-square and NSE are larger than 0.91 and 0.78, respectively, meaning that the average value of the statistics and the simulated yield are close. The values of PBIAS are less than ±20% of the average statistical yield. Therefore, the EPIC model can accurately simulate maize yield at the global scale.

3.3 Establishment of the Drought Vulnerability Curve for Maize

The maize drought vulnerability curve quantifies the yield loss in response to different *DHI*s. The curve can be built by simulating the drought stress and yield under hypothetical irrigation scenarios. In the optimal scenario, the potential yield is achieved when the water stress is 0 during the growing season. In the killing scenario, the crop is killed and the water stress is 1. The water stress and crop yields under different hypothetical irrigation scenarios with a daily time step were simulated. Then, we calculated the *DHI*s and yield loss ratio and fitted the maize drought vulnerability curves for the 35 maize-planting zones (Yin et al. 2014).

3.4 Evaluation of the GEPIC-Vulnerability-Risk Model

The GEPIC-V-R model was evaluated by comparing the simulated expected maize yield loss ratio from drought and the actual maize yield loss ratio during the reference period (1971–2000). By forcing the risk assessment model with meteorological data for the reference period, the *DHI* and the maize yield loss ratio from drought were simulated for each 0.5° × 0.5° grid cell. The *DHI* for each grid cell was calculated using Eq. 2. The maximum value of *DHI* is 1, and the minimum is 0.

$$DHI_j = \frac{\sum_{i=1}^{n} WS_{ji}}{\max\limits_{1 \le j \le 30}\left\{\sum_{i=1}^{n} WS_{ji}\right\}} \tag{2}$$

where DHI_j refers to the drought hazard index for year j; WS_{ji} refers to the water stress for day i in year j; and n denotes the number of days affected by water stress in year j.

The expected maize yield loss ratio was calculated using Eq. 3.

$$L_{\mathrm{Exp}} = \sum_{i=1}^{m} V(u_i) \times f(u_i) \tag{3}$$

where L_{Exp} is the expected yield loss ratio for the period; $V(u_i)$ is the corresponding yield loss ratio for the sample u_i; $f(u_i)$ is the probability of the sample u_i; m is the number of members in U; and U is a discrete universe of the incomplete dataset *DHI*.

In this study, the length of the period was 30 years. It is impossible to accurately estimate the probability density function based on this small sample size, so information diffusion was used to expand the sample, following Huang (1997). We defined $\mathrm{U} = \{u_1, u_2, u_3, \ldots, u_n\}$, and assumed the resolution of U to be 0.001 (that is, $\mathrm{U} = \{0, 0.001, 0.002, \ldots, 1\}$). The normal information diffusion equation (Eq. 4) was used to diffuse the information carried by *DHI* to u_i.

$$f_j(u_i) = \frac{1}{h\sqrt{2\pi}} \exp\left[-\frac{\left(DHI_j - u_i\right)^2}{2h^2}\right] \tag{4}$$

where DHI_j is a given sample, and u_i is the controlling point. The normal diffusion coefficient h was calculated using Eq. 5:

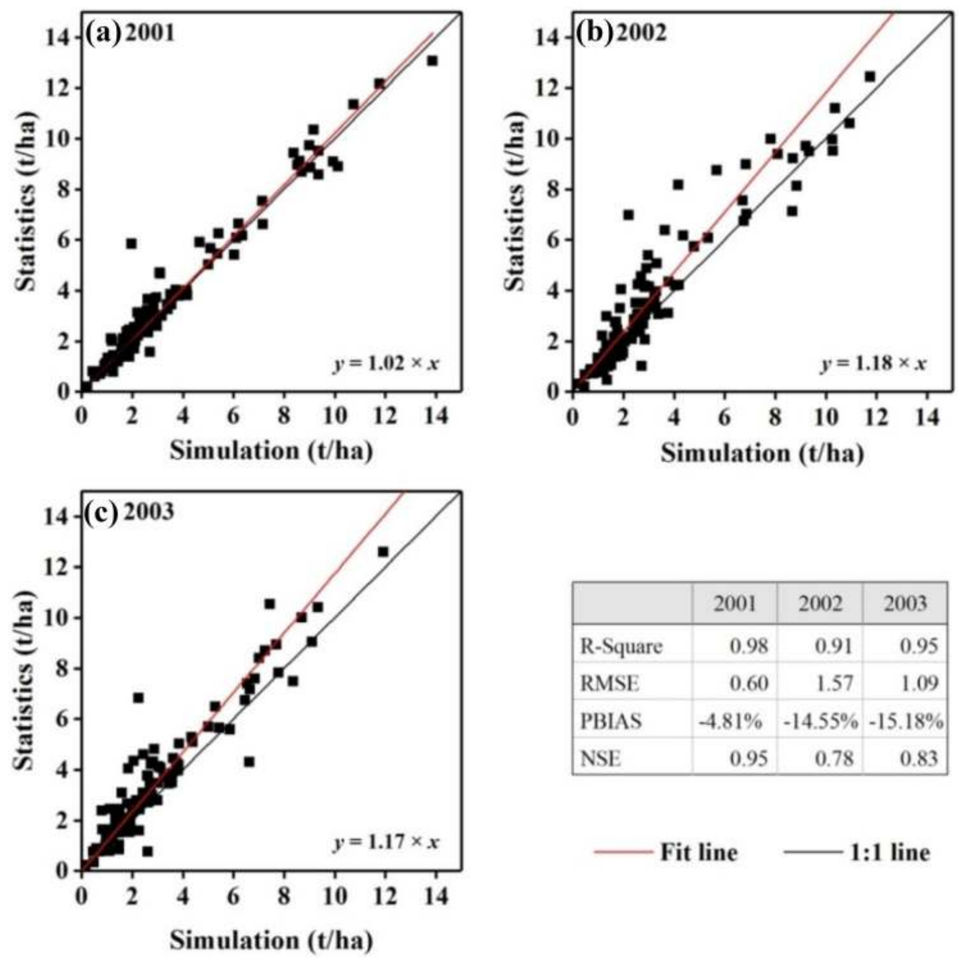

	2001	2002	2003
R-Square	0.98	0.91	0.95
RMSE	0.60	1.57	1.09
PBIAS	-4.81%	-14.55%	-15.18%
NSE	0.95	0.78	0.83

Fig. 2 Comparison of maize yields from maize-planting countries around the world between the statistics and the simulation results

$$h = \begin{cases} 0.8146(b-a)\,(n=5) \\ 0.5960(b-a)\,(n=6) \\ 0.4560(b-a)\,(n=7) \\ 0.3860(b-a)\,(n=8) \\ 0.3362(b-a)\,(n=9) \\ 0.2986(b-a)\,(n=10) \\ 2.8651\dfrac{b-a}{n-1}\,(n \geq 11) \end{cases} \tag{5}$$

where $b = \max_{1 \leq i \leq n}\{DHI_i\}$, $a = \min_{1 \leq i \leq n}\{DHI_i\}$, and n is the number of *DHI* samples (n = 30 in this study).

The normalized information distribution of DHI_j sample ($\upsilon(DHI_j, u_i)$) was calculated using Eq. 6.

$$\upsilon(DHI_j, u_i) = \frac{f_j(u_i)}{C} \tag{6}$$

where C refers to the information accumulation of the sample, which is calculated using Eq. 7:

$$C = \sum_{i=1}^{n} f(u_i) \tag{7}$$

The probability $p(u_j)$ of the monitoring sample u_j was calculated from Eq. 8, allowing the probability distribution functions for drought hazard intensity and disaster risk to be estimated.

$$p(u_j) = \frac{\sum_{j=1}^{m} \upsilon(DHI_j, u_i)}{\sum_{j=1}^{m} q(u_j)} \tag{8}$$

The actual maize yield loss ratio was calculated using the losses caused by drought and the crop sown area, following Xu et al. (2011). Twenty-six major planting provinces in China were selected to calculate the actual maize yield loss ratio due to drought. The losses caused by drought, including the covered areas, affected areas, and areas of total crop failure, were obtained from the Ministry of Civil Affairs of China. The crop sown area data were downloaded from the website of the National Bureau of

Statistics of China.[6] There was a significant positive relationship between the simulated maize loss ratio and the actual maize loss ratio (Table 2). The coefficients of the Spearman, Kendall, and Pearson correlation were 0.83, 0.63, and 0.85, respectively, significant at $p < 0.01$. The results show that the risk assessment model can accurately simulate the maize yield loss risk from drought. Therefore, we consider that the GEPIC-V-R model and the drought vulnerability curves of maize are appropriate for assessing maize drought risk under 1.5 °C warming.

3.5 Quantification of the Maize Drought Risk under Climate Change

Quantifying maize drought risk under the effects of climate change includes two steps: calculation of the future maize drought hazard index, and calculation of the future maize drought risk. Future water stress was simulated by using the climate data projected for a selected period to force the GEPIC-V-R model. The *DHI* was calculated using Eq. 2. Future maize drought risk was estimated based on the *DHI* probability distribution function for a selected period, and the maize drought vulnerability curve. We adopted two commonly used indicators of risk to quantify future crop drought risk—the loss ratio corresponding to various return periods (Khare et al. 2015; Davis and Uryasev 2016), and the expected loss ratio (Eq. 3). The loss ratio corresponding to a given annual recurrence interval (ARI) was derived as follows: (1) the hazard map for the return period was estimated using Eq. 9; and (2) the *DHI* at each grid was combined with a vulnerability curve to calculate the loss ratio corresponding to the return period (Eq. 10).

$$DHI_{ARI} = f^{-1}\left(1 - \frac{1}{ARI}\right) \tag{9}$$

$$L_{ARI} = DHI_{ARI} \times V\{\langle L, h\rangle\} \tag{10}$$

where DHI_{ARI} is *DHI* of the annual recurrence interval. We selected two annual recurrence intervals, that is, 5-year and 20-year return periods.

3.6 Statistical Analysis

Investigating differences in maize yield loss ratio from drought between a 1.5 °C warming scenario and the reference period helps in establishing appropriate preventive and adaptive planning strategies for drought. We calculated the loss ratio both globally and in six maize-planting countries: Brazil, China, India, Russia, Ukraine, and the United States, respectively. The difference in maize yield loss ratio from drought of a region is defined as the average of all grids in the region. The distribution of loss ratio differences in each region is summarized through a kernel density plot. To detect changes in annual maize drought loss ratio, we investigated the statistical significance of changes in the ratio between two time series for each maize grid using a two-sample Kolmogorov-Smirnov (K-S) test (Press and Teukolsky 1988).

4 Global Maize Drought Risk at 1.5 °C Warming World

As the temperature had risen + 0.46 °C from the pre-industrial period to the 1971−2000 period (Vautard et al. 2014), the 1.5 °C warming is equivalent to an additional

Table 2 Correlation between the simulated and actual maize yield loss ratios in 26 provinces in China

			Actual	Simulated
Pearson	Correlation Coefficient	Actual	1.00	0.85**
	Sig. (2-tailed)			0.00
	Correlation Coefficient	Simulated	0.85**	1.00
	Sig. (2-tailed)		0.00	
Kendall's tau_b	Correlation Coefficient	Actual	1.00	0.63**
	Sig. (2-tailed)			0.00
	Correlation Coefficient	Simulated	0.63**	1.00
	Sig. (2-tailed)		0.00	
Spearman's rho	Correlation Coefficient	Actual	1.00	0.83**
	Sig. (2-tailed)			0.00
	Correlation Coefficient	Simulated	0.83**	1.00
	Sig. (2-tailed)		0.00	

**Correlation is significant at the 0.01 level (2-tailed).

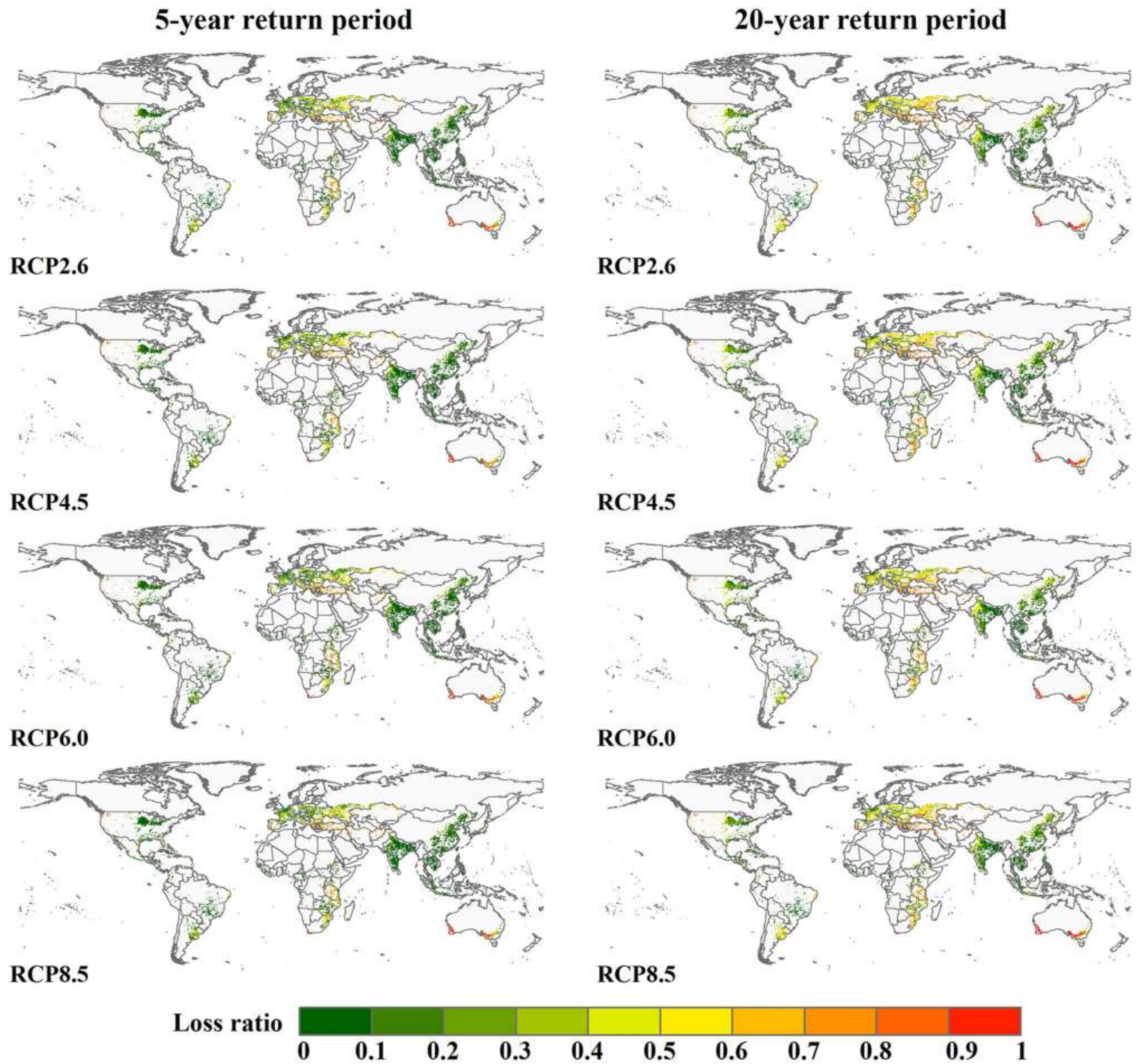

Fig. 3 Maize loss ratio from drought with 5-year (left) and 20-year (right) return periods under different Representative Concentration Pathways (RCPs) for 1.5 °C warming. Red areas have a higher risk of maize drought, indicating that drought can lead to a higher yield loss ratio of maize in these regions, whereas green areas have a lower risk, indicating that maize in these areas would be less affected by drought.

1.04 °C increase above the reference period level. The + 1.5 °C time slice was bounded by the +/− 15-year periods surrounding the central year when the 30-year running mean crossed the +1.5 °C threshold. The time slices for RCP2.6 and RCP8.5 are 2023−2052 and 2021−2050 respectively, while the slices for both RCP4.5 and RCP6.0 are 2026−2055.

The maize loss ratios from droughts with 5-year and 20-year return periods (Eq. 10) under different RCPs for 1.5 °C warming are shown in Fig. 3. The median global average loss ratio increases at longer return periods, from 25% at the 5-year return period to 35% at the 20-year return period. Globally, areas with a high loss ratio from drought (red zone) are mainly located at 40°N−50°N and close to 20°S, including Ukraine, Kazakhstan, Turkey, Spain, Iran, Iraq, Tanzania, South Africa, Australia, the mid-western United States, and northwestern China. The area subject to severe maize drought is projected to gradually increase with increasing return periods, whereas the area experiencing light drought is projected to decrease. For the 5-year and 20-year return periods, areas affected by extremely severe and severe maize drought (loss ratio larger than 0.5) account for 14.57% and 24.98% of the global total maize-planting area, respectively, whereas

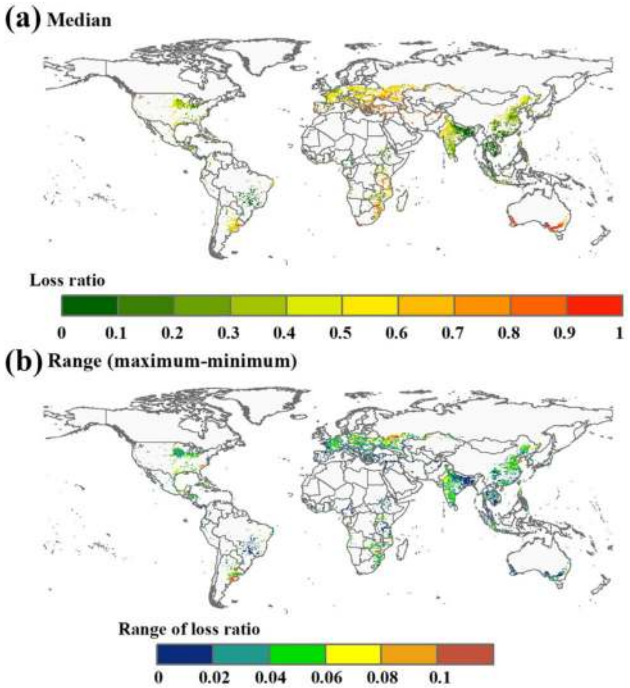

Fig. 4 Median **a** and range **b** of the expected annual maize yield loss ratio from drought across the four Representative Concentration Pathways (RCPs) under 1.5 °C warming

areas affected by extremely light (loss ratio less than 0.1) drought account for 48.07% and 30.31%, respectively.

The global median of expected annual maize yield loss ratios from drought under the four RCPs is 0.41, but the expected yield loss ratios vary significantly among regions and RCPs (Fig. 4a). The areas with high yield loss ratio (red zone) are located in the midlatitudes, primarily central Asia, western and central Europe, Australia, southeastern Africa, and northwestern China. Regions with low loss ratio are mainly located in the lower latitudes. Western Africa has the lowest average loss ratio (0.08), whereas Australia and New Zealand have the highest ratio (> 0.8). Areas affected by light and extremely light drought (loss ratio less than 0.4) comprise approximately 50% of the total maize-planting area in the world, whereas areas affected by extremely severe (loss ratio ranging from 0.8 to 1) and severe (loss ratio ranging from 0.6 to 0.8) drought comprise 8% and 17%, respectively. Nevertheless, due to the main differences related to the magnitude and spatial extent of climatic factors (Taylor et al. 2013), the range (maximum minus minimum) of expected annual maize yield loss ratio from drought across the four RCPs (representing future scenario uncertainty) varies significantly among regions (Fig. 4b). The expected annual maize yield loss ratio is projected to vary slightly (dark blue zone, range < 0.02) among RCP scenarios in Brazil, western United States, Spain, Turkey, Iran, Afghanistan, northeast India, Australia, Southeast Asia, and the Sichuan Basin in China. Therefore, in those regions, climate risk mitigation has a relatively small potential impact on drought risks (Taylor et al. 2013), and the uncertainty associated with RCP scenarios is negligible. The areas with an extremely broad range of loss ratios (red zone, range ≥ 0.1) across the four RCP scenarios are located in Argentina, Russia, Zambia, and northeast China; in these regions, the potential impacts of different climate risk mitigation approaches on drought risk show some notable differences.

The value and distribution of the differences in the expected annual maize yield loss ratio between the 1.5 °C warming scenario and 1971–2000, under different RCPs both globally and in the six selected maize-planting countries, are shown in Fig. 5. The differences under higher emission scenarios are generally higher than those under lower emission scenarios, and the median difference of the average global maize yield loss ratio under 1.5 °C warming is − 0.93%, meaning that the climate change could reduce the global maize drought risk. The differences in expected annual yield loss ratio in the world have a relatively "normal" distribution, which shows that an overwhelming majority of the global maize-planting grids have a relatively small yield loss ratio difference (− 10% ≤ difference ≤ 10%), with only very few grids having very large differences (an absolute difference larger than 20%). The difference is projected to be negative in China and India, but positive in the four other major maize-planting countries; the maize drought is expected to intensify in these four countries under a 1.5 °C warming. Those countries identified in this study as facing increased risk are broadly consistent with those identified in previous analyses (Leng and Hall 2019), except for India and China where this study suggested a slight decrease while a previous study suggested an increase (Leng and Hall 2019). The differences in yield loss ratio in five of the maize-planting countries have relatively "normal" distributions, except for Ukraine. For Brazil, China, and the United States, an overwhelming majority of maize-planting grids have a relatively small difference in yield loss ratio. The difference is less than 0 in most maize-planting grids in India, whereas it is larger than 0 in a small majority of maize-planting grids in Ukraine.

Figure 6 shows the fraction of the maize-planting area experiencing a statistically significant difference of annual maize yield loss ratio from drought under 1.5 °C warming compared to the loss ratio in the reference period in the world and each maize-planting country under different RCPs. Approximately 26% of the global maize-planting area is projected to have significant change in maize yield loss ratio from drought. The area with a significant change in yield loss ratio increases from RCP2.6 to RCP8.5. The order of the RCP scenarios in terms of the fraction of the

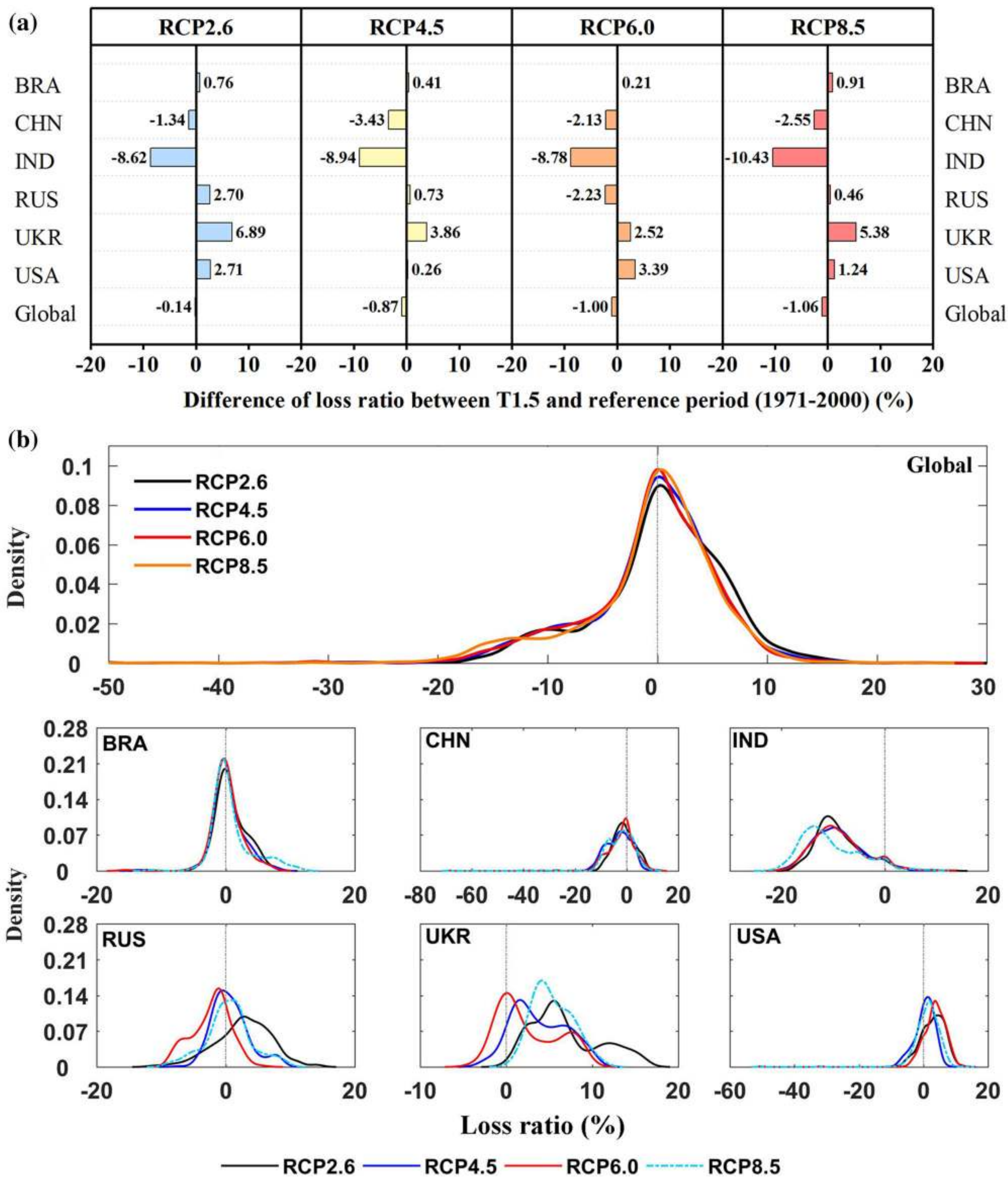

Fig. 5 Difference in expected annual maize yield loss ratio from drought between the 1.5 °C warming scenario and the 1971−2000 period: **a** and kernel density plot highlighting the distribution of the difference; **b** in six major maize-planting countries and globally under different Representative Concentration Pathways (RCPs). BRA, CHN, IND, RUS, UKR, and USA are short for Brazil, China, India, Russia, Ukraine, and the United States, respectively.

maize-planting area experiencing a statistically significant statistical change, from the largest to the smallest, is RCP6.0 (32.40%), RCP4.5 (26.58%), RCP8.5 (26.00%), and RCP2.6 (16.00%). The fraction of the maize-planting area with a significant change is the largest in China, with a median of 47.37%. India would have the smallest fraction

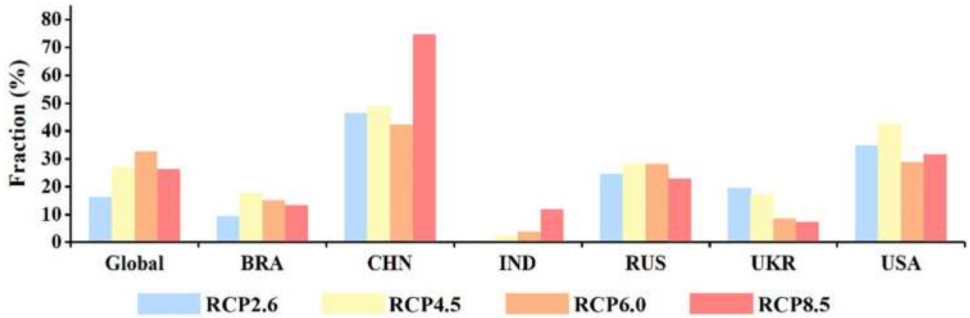

Fig. 6 Fraction of the maize-planting area experiencing a statistically significant difference of annual maize yield loss ratio from drought under 1.5 °C warming, compared to the loss ratio in the reference period in the world and each maize-planting country under different Representative Concentration Pathways (RCPs). BRA, CHN, IND, RUS, UKR, and USA are short for Brazil, China, India, Russia, Ukraine, and the United States, respectively.

of its maize-planting area experiencing a significant change, with a median of 2.79%.

5 Discussion

Based on the GEPIC-V-R model, a global-scale, future-oriented risk assessment framework is proposed. In this framework, the spatial scale is a 0.5° × 0.5° grid, and the GEPIC-V-R model can be validated by comparing multivariate model output (for example, yield, simulated loss ratio) and observational data (for example, yield, losses caused by drought, and previous studies). However, the estimate in grid unit is more computationally expensive and needs more data to calibrate the crop model to ensure simulation accuracy, and the reasons why we selected the 0.5° × 0.5° grid are as follows. Due to the substantial area difference among regions and countries, a large area could conceal intra-regional disparity, exaggerate visual impression, and even lead to wrong perception. Maize is not distributed over an entire country area or region. The gridded risk estimates have the flexibility to aggregate risk estimates into different spatial units. They can be aggregated over various levels of administrative units, but also over areal units that do not follow administrative boundaries, such as river basins, enabling integration and analyses with a range of other spatial datasets. Thus, by demonstrating the spatial variation across the global 0.5° × 0.5° grid, the proposed framework can provide scientific evidence for the development of local agricultural drought risk reduction management strategies.

In the proposed framework, projection of drought risk under climate change contains uncertainties associated with two key sources—crop modeling and GCM output (Orlowsky and Seneviratne 2013; Asseng et al. 2015; Lu et al. 2019). First, the EPIC model uses more than 50 crop parameters to simulate more than 100 types of crops (Williams et al. 1989), and the performance of the model largely depends on the parameterizations of crop varieties and agricultural management factors (for example, planting date and irrigation) (Yao et al. 2011; Leng and Hall 2020). Given that regional information on strongly spatially-heterogeneous parameterizations is scarce, there is larger uncertainty on a regional scale than on a site scale (Yao et al. 2011). To reduce uncertainty, it is feasible to calibrate and validate the genetic parameters in the crop model zone by zone through comparing the simulated and statistical yield (Yin et al. 2014). In this study, comparing the simulation results with national maize yield statistics (2001–2003) demonstrated that the calibrated EPIC model can accurately simulate global yield. To ensure the accuracy of the simulated risk, we compared the simulated expected loss ratio with statistics in China. The three correlation coefficients (Spearman, Kendall, and Pearson) were all more than 0.6, showing that the spatial pattern of maize yield loss risk from drought could be reproduced well by the GEPIC-V-R model during the reference period. Therefore, the reliability of global maize drought risk assessment under climate change can be guaranteed. While the process-based model can well reproduce the patterns of yield variability of maize, there are substantial biases in predictions of year-to-year variability and average of yield. Machine learning methods perform well in reproducing the average and probability distribution of yield (Leng and Hall 2020). Therefore, the machine learning algorithm could be supplementary to the framework.

Second, when future climate projections from a GCM are used to force a crop model, climate model uncertainties may be amplified. The multiple GCMs and/or multiple crop models ensemble (MME) has been widely used to assess the impacts of climate change on agricultural production (Asseng et al. 2015; Yin et al. 2015; Rodríguez et al. 2019). These studies found that variability between individual models is large but the ensemble median and mean appear to be good predictors (Wallach et al. 2018). However, the MME method is very computationally expensive.

Therefore, in the case study, we applied one combination of GCM/crop model instead of a multiple GCM/multiple crop model to demonstrate the validity of the proposed methodology/framework in a global crop drought risk assessment.

Maize drought risk stems from the interaction of drought hazard, vulnerability, and exposure (IPCC 2012, 2014). The risk is not static, but rather dynamic under climate change, depending on changes of these three factors (Poljanšek et al. 2017). In this case study, drought hazard is derived from an information diffusion analysis of a 30-year water stress time series in the maize-growing period for a 1.5 °C warming. Physical vulnerability is an inherent property of maize, and depends on the maize variety. Adopting drought tolerant maize varieties is one of the important strategies for climate change adaptation, especially in semiarid and arid regions (Cairns et al. 2013; Takim 2017); however, improvement of maize varieties was not considered in this study and could result in the overestimation of maize physical drought vulnerability under climate change in some regions. Vulnerability is determined not only by physical vulnerability but also by social and environmental factors (Wang et al. 2013; Poljanšek et al. 2017). For example, CO_2 is not only a major cause for climate warming but also an important environmental factor in determining the vulnerability. Elevated CO_2 fertilizes the crop and alleviates the negative impact of drought and vulnerability (Ottman et al. 2001; Wang et al. 2017; Bhargava and Mitra 2021). Therefore, the risk may be overestimated in this study because the elevated CO_2 was not considered.

In this framework, the exposure of maize to drought is defined as those maize-planting areas located in drought-prone areas (UNISDR 2009; Carrão et al. 2016; Alamgir et al. 2019). The maize-planting areas under 1.5 °C warming were kept the same as those in the reference period, and the exposure was assumed to be equal to unity at the 0.5° resolution (Yin et al. 2014). However, climate change and variability could alter the geographically suitable areas for maize (Ramirez-Cabral et al. 2017; Kogo et al. 2019). Globally, the tropics of Cancer and Capricorn indicate the highest loss of climatic suitability, in contrast to high-altitude and high-latitude regions that exhibit an increase of suitability (Ramirez-Cabral et al. 2017; Ji et al. 2018). The higher average temperatures also have the potential to accelerate the phenological development of maize (Chen and Liu 2014; Hatfield and Dold 2018). Furthermore, physical vulnerability varies in response to climate change across phenological development stages (Wilson et al. 1995; Pan et al. 2017). Therefore, to improve the future-oriented risk assessment of agricultural drought under climate change, future studies should consider the dynamics of exposure and vulnerability alongside climate variability (Hagenlocher et al. 2019; Meza et al. 2020).

6 Conclusion

With support of the GEPIC-V-R model, an analytical framework and associated methods for quantifying the future global-scale maize drought risk at the resolution of 0.5° × 0.5° have been proposed in this study. The analytical framework comprises four major steps: calibration and validation of the EPIC model, drought vulnerability curve establishment, evaluation of the GEPIC-V-R model, and quantification of crop drought risk under climate change. In this framework, the GEPIC-V-R model can be calibrated and validated using datasets from in situ observations and previous studies, and the water stress and drought risk under climate change can then be simulated accurately.

In a 1.5 °C warming world, the expected annual maize yield loss ratio from drought is about 0.41. The maize drought risk in midlatitude regions is projected to be high, and regions with low loss ratio are mainly located in the lower latitudes. Globally, the median average loss ratio increases at longer return periods, and a warming of 1.5 °C would lead to only slight decreases (− 0.93%) in maize yield from drought.

Because drought vulnerability and exposure are not static, but rather dynamic under climate change, future maize drought risk assessment needs to consider the patterns and dynamics of exposure and vulnerability alongside climate change and variability. Furthermore, different maize varieties and phenological stages present different sensitivities to drought. Future studies should pay greater attention to assessing the drought risk across different maize varieties and phenological stages.

Acknowledgements This work was supported by the National Natural Science Foundation of China (Grant No. 41671501, 41901046, and 91747201). The bias-corrected and downscaled projection data of HadGEM2-ES were obtained from the Inter-Sectoral Impact Model Inter-comparison Project (ISI-MIP) Earth System Grid Federation (ESGF) Node (http://esg.pik-potsdam.de). We acknowledge the ISI-MIP coordination team for the model outputs.

References

Alamgir, M., M. Mohsenipour, R. Homsi, X. Wang, S. Shahid, M. Shiru, N. Alias, and A. Yzir. 2019. Parametric assessment of seasonal drought risk to crop production in Bangladesh. *Sustainability* 11(5): Article 1442.

Asseng, A., F. Ewert, P. Martre, R.P. Rötter, D.B. Lobell, D. Cammarano, B.A. Kimball, M.J. Ottman, et al. 2015. Rising temperatures reduce global wheat production. *Nature Climate Change* 5: 143−147.

Batjes, N.H. (ed.). 2000. Global Soil Profile Data (ISRIC-WISE). ORNL Distributed Active Archive Center, Oak Ridge National Laboratory, Oak Ridge, Tennessee, USA. http://www.daac.ornl.gov. Accessed 9 Nov 2019.

Bhargava, S., and S. Mitra. 2021. Elevated atmospheric CO_2 and the future of crop plants. *Plant Breeding* 140(1): 1−11.

Boote, K.J., J.W. Jones, and N. Pickering. 1996. Potential uses and limitations of crop models. *Agronomy Journal* 88(5): 704−716.

Boote, K.J., J.W. Jones, J.W. White, S. Asseng, and J.I. Lizaso. 2013. Putting mechanisms into crop production models. *Plant, Cell & Environment* 36(9): 1658−1672.

Cairns, J., J. Hellin, K. Sonder, J. Araus, J. MacRobert, C. Thierfelder, and B. Prasanna. 2013. Adapting maize production to climate change in sub-Saharan Africa. *Food Security* 5(3): 346−360.

Cardona, O., M. van Aalst, J. Birkmann, M. Fordham, G. McGregor, R. Perez, R.S. Pulwarty, E.L.F. Schipper, et al. 2012. Determinants of risk: Exposure and vulnerability. In *Managing the risks of extreme events and disasters to advance climate change adaptation*, ed. C. Field, V. Barros, T. Stocker, D. Qin, D.J. Dokken, K.L. Ebi, M.D. Mastrandrea, K.J. Mach, et al., 65−108. Cambridge, UK: Cambridge University Press.

Carrão, H., G. Naumann, and P. Barbosa. 2016. Mapping global patterns of drought risk: An empirical framework based on sub-national estimates of hazard, exposure and vulnerability. *Global Environmental Change* 39: 108−124.

Chen, P., and Y. Liu. 2014. The impact of climate change on summer maize phenology in the northwest plain of Shandong province under the IPCC SRES A1B scenario. *IOP Conference Series: Earth and Environmental Science* 17(1): Article 012053.

Cui, D. 1994. *Agricultural climate and crop climate of the world*. Hangzhou, China: Press of Zhejiang Science and Technology (in Chinese).

Dai, A. 2013. Increasing drought under global warming in observations and models. *Nature Climate Change* 3: 52–58.

Davis, J., and S. Uryasev. 2016. Analysis of tropical storm damage using buffered probability of exceedance. *Natural Hazards* 83(1): 465–483.

Dike, V., M. Shimizu, M. Diallo, Z. Lin, O. Nwofor, and T. Chineke. 2015. Modelling present and future African climate using cmip5 scenarios in HadGEM2-ES. *International Journal of Climatology* 35(8): 1784–1799.

Döll, P., and S. Siebert. 2002. Global modeling of irrigation water requirements. *Water Resources Research* 38(4): Article 1037.

Elliott, J., C. Müller, D. Deryng, J. Chryssanthacopoulos, K.J. Boote, M. Büchner, I. Foster, M. Glotter, et al. 2015. The global gridded crop model intercomparison: Data and modeling protocols for Phase 1 (v1.0). *Geoscientific Model Development* 8: 261−277.

FAO (Food and Agriculture Organization of the United Nations). 2015. *The impact of natural hazards and disasters on agriculture and food security and nutrition: A call for action to build resilient livelihoods*. http://www.fao.org/emergencies/resources/documents/resources-detail/en/c/280784/. Accessed 18 Apr 2021.

Franke, J., C. Müller, J. Elliott, A. Ruane, J. Jägermeyr, J. Balkovic, P. Ciais, M. Dury, et al. 2020. The GGCMI Phase 2 experiment: Global gridded crop model simulations under uniform changes in CO_2, temperature, water, and nitrogen levels (protocol version 1.0). *Geoscientific Model Development* 13: 2315−2336.

Guo, H., X. Zhang, F. Lian, Y. Gao, D. Lin, and J. Wang. 2016. Drought risk assessment based on vulnerability surfaces: A case study of maize. *Sustainability* 8(8): Article 813.

Hagenlocher, M., I. Meza, C. Anderson, A. Min, F.G. Renaud, Y. Walz, S. Siebert, and Z. Sebesvari. 2019. Drought vulnerability and risk assessments: State of the art, persistent gaps, and research agenda. *Environmental Research Letters* 14(8): Article 083002.

Hartkamp, A., J. White, A. Aguilar, M. Bänziger, G. Srinivasan, G. Granados, and J. Crossa. 2001. Maize production environments revisited: A GIS-based approach. Mexico: CIMMYT Natural Resources Group.

Hatfield, J.L., and C. Dold. 2018. Climate change impacts on corn phenology and productivity. In *Corn—Production and human health in changing climate*, ed. Amanullah and Shah Fahad, 95−114. London: IntechOpen.

Hoegh-Guldberg, O., D. Jacbo, M. Taylor, M. Bindi, S. Brown, I. Camilloni, A. Diedhiou, R. Djalant, et al. 2018. Impacts of 1.5°C global warming on natural and human systems. In *Global warming of 1.5°C. An IPCC special report on the impacts of global warming of 1.5°C above pre-industrial levels and related global greenhouse gas emission pathways, in the context of strengthening the global response to the threat of climate change, sustainable development, and efforts to eradicate poverty*, ed. V. Masson-Delmotte, P. Zhai, H.-O. Pörtner, D. Roberts, J. Skea, P.R. Shukla, A. Pirani, W. Moufouma-Okia, et al., 175−311. Geneva: IPCC.

Huang, C. 1997. Principle of information diffusion. *Fuzzy Sets and Systems* 91(1): 69−90.

IPCC (Intergovernmental Panel on Climate Change). 2012. *Managing the risks of extreme events and disasters to advance climate change adaptation. A special report of working groups I and II of the Intergovernmental panel on climate change*. Cambridge and New York: Cambridge University Press.

IPCC (Intergovernmental Panel on Climate Change). 2013. Summary for policymakers. In *Climate change 2013: The physical science basis*. Contribution of Working Group I to the fifth assessment report of the Intergovernmental Panel on Climate Change. Cambridge and New York: Cambridge University Press.

IPCC (Intergovernmental Panel on Climate Change). 2014. *Climate change 2014: Synthesis report*. Contribution of working groups I, II and III to the fifth assessment report of the Intergovernmental Panel on Climate Change, ed. Core writing team, R.K. Pachauri, L.A. Meye. Geneva: IPCC.

Ji, Y., G. Zhou, Q. He, and L. Wang. 2018. The effect of climate change on spring maize (*Zea mays L.*) suitability across China. *Sustainability* 10(10): Article 3804.

Khare, S., A. Bonazzi, C. Mitas, and S. Jewson. 2015. Modelling clustering of natural hazard phenomena and the effect on re/insurance loss perspectives. *Natural Hazards and Earth System Sciences* 15(6): 1357−1370.

Kogo, B., L. Kumar, R. Koech, and C. Kariyawasam. 2019. Modelling climate suitability for rainfed maize cultivation in Kenya using a Maximum Entropy (MaxENT) approach. *Agronomy* 9(11): Article 727.

Leng, G., and J. Hall. 2019. Crop yield sensitivity of global major agricultural countries to droughts and the projected changes in the future. *Science of the Total Environment* 654: 811−821.

Leng, G., and J. Hall. 2020. Predicting spatial and temporal variability in crop yields: An inter-comparison of machine learning, regression and process-based models. *Environmental Research Letters* 15(4): Article 044027.

Liu, J. 2009. A GIS-based tool for modeling large-scale crop-water relations. *Environmental Modelling & Software* 24(3): 411−422.

Lu, J., G. Carbon, and J. Grego. 2019. Uncertainty and hotspots in 21st century projections of agricultural drought from CMIP5 models. *Scientific Reports* 9(1): Article 4922.

Meza, I., S. Siebert, P. Döll, J. Kusche, C. Herbert, E.E. Rezaei, H. Nouri, and H. Gerdener et al. 2020. Global-scale drought risk assessment for agricultural systems. *Natural Hazards and Earth System Sciences* 20(2): 695–712.

Orlowsky, B., and S.I. Seneviratne. 2013. Elusive drought: Uncertainty in observed trends and short- and long-term CMIP5 projections. *Hydrology and Earth System Sciences* 17: 1765−1781.

Ottman, M. J., B.A. Kimball, P.J. Pinter, G.W. Wall, R.L. Vanderlip, S.W. Leavitt, R.L. LaMorte, A.D. Matthias, et al. 2001. Elevated CO_2 increases sorghum biomass under drought conditions. *New Phytologist* 150(2): 261−273.

Pan, D., H. Jia, W. Zhang, and Y. Yin. 2017. Research on maize drought vulnerability based on field experiments. *Journal of Catastrophology* 32(2): 150−153 (in Chinese).

Poljanšek, K., M. Marin Ferrer, T. De Groeve, and I. Clark. 2017. *Science for disaster risk management 2017: Knowing better and loosing less*. EUR 28034 EN. Luxembourg: Publications Office of the European Union.

Press, W.H., and S.A. Teukolsky. 1988. Kolmogorov-Smirnov test for two-dimensional data. *Computers in Physics* 2(4): 74−77.

Ramankutty, N., A.T. Evan, C. Monfreda, and J.A. Foley. 2008. Farming the planet: 1. Geographic distribution of global agricultural lands in the year 2000. *Global Biogeochemical Cycles* 22: Article GB1003.

Ramirez-Cabral, N., L. Kumar, and F. Shabani. 2017. Global alterations in areas of suitability for maize production from climate change and using a mechanistic species distribution model (CLIMEX). *Scientific Reports* 7: Article 5910.

Rodríguez, A., M. Ruiz-Ramos, T. Palosuo, T.R. Carter, S. Fronzek, I.J. Lorite, R. Ferrise, N. Pirttioja, et al. 2019. Implications of crop model ensemble size and composition for estimates of adaptation effects and agreement of recommendations. *Agricultural and Forest Meteorology* 264: 351−362.

Rosenzweig, C., N.W. Arnell, K.L. Ebi, H. Lotze-Campen, F. Raes, C. Rapley, M.S. Smith, W. Cramer, et al. 2017. Assessing intersectoral climate change risks: The role of ISIMIP. *Environmental Research Letters* 12(1): Article 010301.

Schewe, J., J. Heinke, D. Gerten, I. Haddeland, N.W. Arnell, D.B. Clark, R. Dankers, S. Eisner, et al. 2014. Multimodel assessment of water scarcity under climate change. *Proceedings of the National Academy of Sciences of the United States of America* 111(9): 3245−3250.

Schneiderbauer, S., E. Calliari, U. Eidsvig, and M. Hagenlocher. 2017. The most recent view of vulnerability. In *Science for disaster risk management 2017: Knowing better and loosing less*, ed. K. Poljanšek, M. Marín Ferrer, T. De Groeve, and I. Clark, 70−84. Luxembourg: Publications Office of the European Union.

Shi, P. 2012. Atlas of natural disaster risk of China. Beijing, China: Science Press (in Chinese).

Takim, F. 2017. Climate change adaptation options: Importance of drought tolerant maize seeds. UNU-INRA policy brief. Tokyo, Japan: Institute for Natural Resources in Africa, United Nations University.

Taylor, I., E. Burke, L. McColl, P. Falloon, G. Harris, and D. McNeall. 2013. The impact of climate mitigation on projections of future drought. *Hydrology and Earth System Sciences* 17: 2339−2358.

Thornley, J., and I. Johnson. 1990. *Plant and crop modeling: A mathematical approach to plant and crop physiology*. Oxford, UK: The Blackburn Press.

UNDP (United Nations Development Programme). 2005. Reducing disaster risk: A challenge for development. New York: United Nations Development Programme.

UNFCCC (United Nation Framework Convention on Climate Change). 2015. The Paris Agreement Summary. Climate focus client brief on the Paris Agreement III 28 December 2015. Bonn, Germany: UNFCCC.

UNISDR (United Nations International Strategy for Disaster Reduction). 2009. UNISDR terminology on disaster risk reduction (2009). Geneva, Switzerland: UNISDR.

van Vuuren, D.P., J. Edmonds, M. Kainuma, K. Riahi, A. Thomson, K. Hibbard, G.C. Hurtt, T. Kram, et al. 2011. The representative concentration pathways: An overview. *Climatic Change* 109: 5−31.

Vautard, R., A. Gobiet, S. Sobolowski, E. Kjellström, A. Stegehuis, P. Watkiss, T. Mendlik, O. Landgren, et al. 2014. The European climate under a 2°C global warming. *Environmental Research Letters* 9(3): Article 034006.

Wallach, D., P. Martre, B. Liu, S. Asseng, F. Ewert, P. J. Thorburn, M. van Ittersum, P. K. Aggarwal, et al. 2018. Multimodel ensembles improve predictions of crop-environment-management interactions. *Global Change Biology* 24(11): 5072−5083.

Wang, J., X. Zhang, H. Guo, Y. Yin, F. Lian, and P. Shi. 2016. Drought risk assessment and mapping of major crops in the world. Beijing, China: Science Press (in Chinese).

Wang, Q., J. Wu, T. Lei, B. He, Z. Wu, M. Liu, X. Mo, G. Geng, et al. 2014. Temporal-spatial characteristics of severe drought events and their impact on agriculture on a global scale. *Quaternary International* 349: 10−21.

Wang, Y., D. Yan, J. Wang, Y. Ding, and X. Song. 2017. Effects of elevated CO_2 and drought on plant physiology, soil carbon and soil enzyme activities. *Pedosphere* 27(5): 846−855.

Wang, Z., F. He, W. Fang, and Y. Liao. 2013. Assessment of physical vulnerability to agricultural drought in China. *Natural Hazards* 67(2): 645−657.

Warszawski, L., K. Frieler, V. Huber, F. Piontek, O. Serdeczny, and J. Schewe. 2014. The Inter-Sectoral Impact Model Intercomparison Projection (ISI-MIP): Project framework. *Proceedings of the National Academy of Sciences of the United States of America* 111(9): 3228−3232.

Webber, H., F. Ewert, J.E. Olesen, C. Müller, S. Fronzek, A. C. Ruane, M. Bourgault, P. Martre, et al. 2018. Diverging importance of drought stress for maize and winter wheat in Europe. *Nature Communication* 9: Article 4249.

Williams, J., C. Jones, J. Kiniry, and D. Spanel. 1989. The EPIC crop growth model. *Transactions of the ASAE* 32(2): 497−511.

Wilson, D.R., R.C. Muchow, and C.J. Murgatroyd. 1995. Model analysis of temperature and solar radiation limitations to maize potential productivity in a cool climate. *Field Crops Research* 43(1): 1−18.

Xu, X., J. Zheng, Q. Ge, E. Dai, and C. Liu. 2011. Drought risk assessment on regional agriculture: A case in Southwest China. *Progress in Geography* 30(7): 883−890.

Yao, F., P. Qin, J. Zhang, E. Lin, and V. Boken. 2011. Uncertainties in assessing the effect of climate change on agriculture using model simulation and uncertainty processing methods. *Chinese Science Bulletin* 56: 729−737.

Yin, Y., Q. Tang, and X. Liu. 2015. A multi-model analysis of change in potential yield of major crops in China under climate change. *Earth System Dynamics* 6(1): 45−59.

Yin, Y., X. Zhang, D. Lin, H. Yu, J. Wang, and P. Shi. 2014. GEPIC-V-R model: A GIS-based tool for regional crop drought risk assessment. *Agricultural Water Management* 144: 107−119

Yu, C., X. Huang, H. Chen, G. Huang, S. Ni, J.S. Wright, J. Hall, P. Ciais, et al. 2018. Assessing the impacts of extreme agricultural droughts in China under climate and socioeconomic changes. *Earth's Future* 6(5): 689−703.

Yue, Y., L. Wang, J. Li, and A. Zhu. 2018. An EPIC model-based wheat drought risk assessment using new climate scenarios in China. *Climatic Change* 147: 539−553.

Zeng, J., R. Zhang, Y. Lin, X. Wu, J. Tang, P. Guo, J. Li, and Q. Wang. 2020. Drought frequency characteristics of China, 1981−2019, based on the vegetation health index. *Climate Research* 81: 131−147.